Implementation of Satellite Road Image Denoising using Iterative Domain Guided Image Filtering with Gray World Optimization

D. Subhashini [1] and V. B. S. Srilatha Indira Dutt[2]
[1] GITAM (Deemed to be University), Visakapatnam, India
[2] Dept of ECE, GITAM (Deemed to be University), Visakapatnam, India
Email: dsubhashini_ece@mgit.ac.in, 1121960404011@gitam.in; svemuri@gitam.edu

***Abstract*—**Generally, Satellite road images are in noisy conditions such as noise, snow, thin cloud, dust, etc., which results in contrast degradations in the image. Denoising is defined as the technique for removing noise or atmospheric impurities from an image to increase the quality of an image. But most of the state of art approaches failed to remove the atmospheric effects and noise from the road image perfectly. To solve this problem, this paper majorly focuses on developing a Gray World Optimization (GWO) algorithm for the perfect estimation of atmospheric road light. The work also develops the novel method for dark channel prior-based transmission map estimation and refinement in pixel-wise and patch-wise manner. Thus, the atmospheric road effects are resolved in each pixel-based patch. Finally, a fast iterative domain guided image filtering (ID-GIF) approach was developed to obtain smoothen output with Denoising properties. The simulation results show that the proposed work provides better quantitative and qualitative results than state-of-the-art approaches.

***Index Terms*—**Gray world optimization, fast iterative domain guided image filtering, dark channel prior

I. Introduction

Roads are identified by human experts, who can update the transport databases easily with the help of tools, such as cartography (e.g., ArcGIS) [1]. However, this manual method is expensive and time-consuming since the scenes are very complex. In addition, it also needs to be updated frequently. Moreover, the quality of the results depends on the experience of a particular study area and skills of the human operator [2] because they can be recognized well even from images having incomplete roads or roads occluded with trees or shadows of high buildings [3]. For the past two decades, many researchers have contributed to automatic and semi-automatic approaches. Due to the extreme complexity of urban road structures [4], automatic road network extraction is a challenging task since the road is in the presence of different substances (vehicles, footpaths, stop lines), different circumstances (urban, highways, off-road), different road categories (shape, color), different imaging conditions (varying illumination, different viewpoints and weather conditions) and different backgrounds (surrounded by trees, residential areas, and plain soil) [5]. An ad-hoc multistage approach is followed by most of the automatic road detections.

Unfortunately, a few samples are used to test the performance of these approaches with multiple thresholds to be tuned. But it is a very complex and challenging task with large real-world datasets (rural, suburban, and developed urban areas). Without human involvement in any of the stages [6], full automation remains vague and weak in the accuracy and completeness of the road network extracted. Since the appearance of roads depends upon the spatial resolution of the satellite images, the automatic approaches produce false positive and true negative results. The accuracy of road extraction is reduced chiefly because of some assumptions [7] made based on the road's geometry to generate the road seed point initially. To find the road seed, the whole image needs to be scanned. Hence, a considerable computation is involved. Ground objects or obstacles, such as trees, buildings, and their shadows, are barriers in the images of roads. Vehicles [8] on the road may cover certain parts of a road and make it difficult to trace the entire road continuously with the same profile. Overall, these factors affect the performance of automated road extraction methodologies.

However, semi-automatic approaches for extracting roads from satellite images are utilizing the computer's computation speed to reduce the time taken by with manual approaches [9], [10], and also getting expert knowledge in critical situations to make decisions for guiding extraction into the right path, since, a linear feature can be a road segment [11], a river segment, the boundary of a house, the boundary of a land parcel and so on. Here, unnecessarily one need not waste time in post-correction by removing erroneous results. So, combining the speed and accuracy of a computer program with the interpretative skill of a human operator achieves quality results, better completeness, and the best robustness. In this method, the user provides the seed point [12].

Semi-automated methods [13], [14] can be classified into two categories. One is called road tracing or linking. A human operator must provide a starting point and direction for a traceable feature such as a road. Then, the algorithms may trace or follow the road from the starting point, based on some radiometric, geometric, or topological characteristics to trace the rest of the road.

Manuscript received November 5, 2021; revised June 15, 2022.
doi:10.12720/jcm.17.6.581-591

The next category is called road linking. Here, a human operator identifies the object of interest (roads in this case) from a digital image and selects a few seed points that are coarsely distributed. The extracted linear features are automatically linked by computer algorithms based on radiometric, geometric, and topological measures.

The solution to this issue is to use specific noise removal algorithms [15] to reduce the attenuation or hike the steadiness and sturdiness of the visual arrangement. To solve this problem, the contributions of this paper are as follows:

- A novel transmission mapping and refining methodology have been developed using dark channel before solving the atmospheric road effects.
- The road atmospheric light estimation is carried out using the novel GWO algorithm; it effectively calculates the noise under various road atmospheric environments.
- Finally, an iterative domain-guided image filtering approach was developed to enhance the image and achieve the smoothening properties.
- The simulations are carried out on both synthetic and real-time datasets such as noisy satellite images, synthesized noisy images, and noisy natural images with indoor and outdoor databases. The results show that the proposed method provides the better visual quality of output image and also provides the enhancive quality metrics compared to the various literature such as ID-CNN, IDERS and TME-MOF respectively.

The rest of the paper is as follows: section deals with the survey of various related works and identifies their problems. Section III deals with a detailed analysis of the proposed methodology with mathematical analysis. Section IV deals with detailed proposed simulation and comparative analysis with various existing works, and finally, Section V concludes the proposed method with possible future enhancements.

II. Literature Survey

This section deals with the various types of road image denoising methods. In [16], the authors implemented the high-resolution vehicle trajectory extraction and denoising using dynamic programming approaches suitable for extracting road segments from low-resolution remote sensing images. Since these kinds of images manifest the roads as lines at the maximum of 1-3 pixels to represent the road's width, roads can be modeled as linear features. Here, to describe the road, we need to provide a few seed points coarsely by the operator, which is a computational complicated.

In [17], authors sequential decision-making process based I-HAZE approach for road image denoising, which is required to search the shortest path of two road seed candidates by expressing in terms of relationships between neighbouring pixels and is linked together by a merit function, by which roads are extracted from initial seed points automatically by maximizing this predefined merit function. But this method is suffering the composite color issues.

In [18], authors defined denoising autoencoders and geometric properties (slow variations in road curvature and linear features with slight intensity changes in subsequent positions). With this profile, searching starts with each vertex around in a window (3x3 or 5x5) to find the maximum of the merit function based on the road profile. Pyramid-shaped sampling is done only for every third pixel to restrict the searching directions. Unfortunately, this traditional approach is not adequate for medium and high-resolution images. Because roads are here visible as ribbon-like structures, not as linear structures. So, here the goal of road extraction methods is fixed with detecting the road center-line.

In [19], authors implemented the IoT-based Image Defogging System with road accident control for the presence of new geo-referenced road segments using an iterative dehazing-convolutional neural network (ID-CNN). A slight modification is needed in the merit function to add the constraint for embedding road edge characteristics. But this modification is insufficient to extract road centerlines that have high curvature. It results in a set of disconnected linear road segments. Moreover, it couldn't provide details of the road's width and shape for denoising. In [20] authors introduced the machine Learning-based data preparation methodology. Unfortunately, the performance of traditional approach mainly depends on the strength of the initial curve, i.e., parameters such as width, intensity values, and convergence.

In [21], the authors introduced the Bounded Total Variation Denoising method with the endpoints of the input curve; so, it fails to detect concave boundaries. Close initialization cannot be provided for all kinds of road networks, especially in road junctions, since the surrounding roads of the junction may have various degrees of curvatures.

In [22], the authors improved the performance by automatically extracting and denoising vehicle trajectory out the unwanted information and noise before extracting the roads from the remote sensing imagery. For example, segmentation and size distribution analysis methods, trivial opening, filling of small holes, and removing or closing the small paths have been applied respectively for road extraction from the classified image. In [23], authors introduced the Spatially Adaptive Atmospheric Point Spread Function with the images' disturbances, such as objects having similar spectral characteristics as road surfaces; the trivial morphological opening is utilized here. But it cannot handle occluded road areas by vehicles, shadows of trees and buildings, and other objects, and cannot remove roads connecting the houses and shorter road parts because of image frames.

In [24], the authors introduced the Photo-realistic simulation for road scene images cleaned and filled by mathematical morphology. Based on the characteristics such as intensity, texture, color, or intensity values of the

reflecting signals, objects are classified into several groups; this process is called segmentation. But this method suffers from low image clarity. In [25], the authors introduced the multiple scattering model for road scenes in road classification and named TME-MOF; these segmented objects are assigned to different predefined classes. Performance of road extraction can be improved by combining segmentation with classification. The classified objects will be complimentary to successive segmentation, or the following classification will also benefit the segmented objects.

In [26], the authors introduced the spatially adaptive atmospheric point spread function approaches to these two techniques for road extraction. The binary image is given as input, and the output is a picture with a road network only (other objects are filtered out).

In [27], authors implemented modified dark channel prior and neighborhood FCM to extract spectral information to train the feed-forward neural network. More false alarms disconnected road segments are there in the final result. Supervised classification of remote sensing data also depends on the number of training samples. In [28], authors implemented the image feature statistics, and defining appropriate reference data is a critical problem for images with different spatial and spectral resolutions. Segmentation is also an expensive process since scanning the whole image is essential for segmentation algorithms and needs to process all the pixels at least once. In [29], the authors implemented the road and non-road pixels by mixed domain and retracted neighborhood using the Iterative Dehazing Method for Single Remote Sensing (IDERS). Next, the classified road pixels were grouped as geometrically homogeneous objects by a region growing. Then, road features were extracted by applying simple thresholding to the shape measurements. Finally, road centerlines were obtained using thinning and vectorization. Though the roads were mapped well, the final result consists of disconnected roads caused by shadows or obstacles.

III. Proposed Method

Denoising is a technique for removing noise or road atmospheric imperfections from an image to improve its quality and make it more appealing to the viewer. Many noise reduction techniques are used to improve the image's quality to eliminate this loss of figures. Image repair and enhancement can be used to eliminate the noise. Picture enhancement is concerned with enhancing an image's contrast (intensity), whereas image re-establishment is concerned with the effective imaging method in noise. Denoising is regarded as an essential process because the attenuation or noise-free photographs are pleasing to the eye, and it may improve computer vision jobs and client photography. Figure 1 depicts a block diagram of an image denoising approach utilized in the suggested methodology. It comprises two primary steps: an estimate of the transmission map and the elimination of ambient light. The following is a thorough description of each stage's operation.

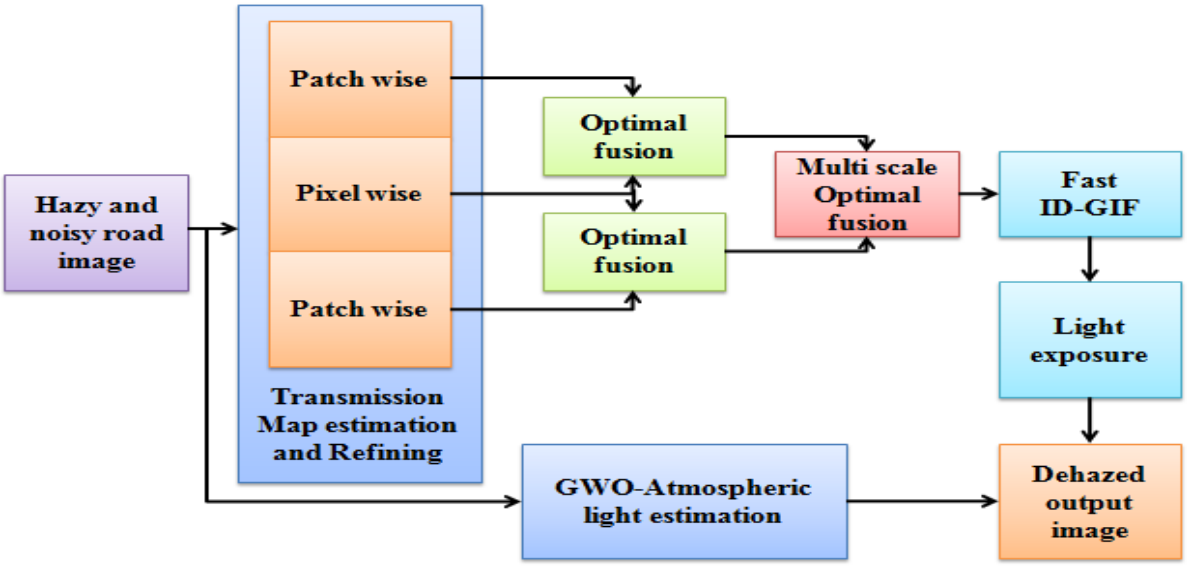

Fig. 1. Proposed hybrid denoising method

A. Transmission Map Estimation and Refining

The components like attenuation and air-light can be interpreted with the help of the next mathematical statement according to koschmieder's law as follows:

$$I(x) = J(x) * t(x) + A * (1 - t(x)) \quad (1)$$

Here, $I(x)$refers to the noisy image, $J(x)$ is the scene radiance or noise-free image respectively. A is the climatic light value, such as global road atmospheric light, and t is the communication channel that specifies the segment of illumination that will not be scattered and grab the receiving picture sensor or camera. Directed depletion is one component of the mathematical

statement $j(x) * t(x)$, while air-light is the other part of the equation $A * (1 - t(x))$. Equation 2 gives $t(x)$ as the transmission map with x as the picture spatial coordinates.

$$t(x) = e^{-\beta\, d(x)} \tag{2}$$

where β is the scene depth and is the road atmospheric scattering coefficient (which is 0 in clear weather). The first term in equation (1), $J(x) * t(x)$, describes a direct attenuation of scene brightness that diminishes exponentially as scene depth rises. The ambient light, or the second term $(1 - t(x))$, on the other hand, rises as the scene depth increases.

Due to the additional ambient light and poor transmission map, noisy pictures are brighter than noise-free images. Because it possesses high-intensity values in extremely dense noise areas, the black channel of a noisy image is an excellent estimate of the noise thickness. As a result, road atmospheric light and transmission maps are calculated using this characteristic.

Transmission map estimation on the noisy input image will be performed in pixel-wise and patch-wise manner. A transmission map gives the extent of light reaching the camera in a degraded image. The dark map derived out of the red channel prior is used to obtain this transmission map. This is the main clue to determine the extent and depth of the noisy image and light transmission in an image formation process. We obtain the equation for the transmission map. In this equation, we introduce a constant parameterα. The equation used for obtaining the transmission map generated by using the dark channel prior is given by

$$t_{pa}(x) = 1 - \alpha \min_{y \in \Omega(x)} \left[\min_{C \in [r,g,b]} \frac{I^c(y)}{A^c} \right] \tag{3}$$

Here, $t_{pa}(x)$is the patch-based transmission map, $(\boldsymbol{x})$ is a local patch centred at $\boldsymbol{x}$ and I^c is a color channel of I. min$\boldsymbol{y}\in(\boldsymbol{x})$ is a minimum filter and min$c\in\{r,g,b\}$ is performed on each pixel in the RGB space. The selection of parameter α is chosen to preserve some amount of noise so that the output image looks natural. A higher value of α results into the complete removal of noise making the image look unrealistic and exhibits colour distorted image whereas the lower value of w results into lower intensity image and makes it darker. The value of α ranges between 0 and 1 in a normalized image. Here, the image is divided into three transmission maps such as two patch wise and one-pixel wise transmission map. Here, the α is used to change the pixel intensities and Ω is used to change the patch size based on the user requirement respectively.

The I^c is a shading channel of j and $\Omega(x)$ is a local patch focused at x. Dark channels are processed utilizing a various patch sizes3×3, 15 x 15 and more. Not many insights are given to characterize the patch size: the probability that the patch contains dark pixels is increased concerning a bigger size. In this manner, the dark channel could be precisely evaluated. In any case, with an enormous patch, the supposition that the transmission is steady in a patch turns out to be less proper, and the hollow artifacts near depth edges become increased. Most transmission mapping-based Denoising strategies figure the dark channel by essentially utilizing a local patch with a fixed size to fundamentally diminish the computation time. It also operates by using a pixel-wise manner.

A portion of the transmission mapping-based lining up strategies thinks about a patch with an alternate size from 15×15, which was fundamentally utilized. The patch size can be progressively adjusted dependent on the image content. In genuine over-satiation, impacts happen in the recovered scene radiance when a tiny patch size is utilized in the first noisy image, including limited light. This prompts a disappointment in the recognizable proof of the environmental light source. A bigger size can resolve this issue, yet it prompts halo effects and black artifacts, particularly along edges. In this manner, two patch sizes of 3×3 and 45×45, which are tentatively recognized, have been utilized in a procedure of transmission mapping.

Incorrect estimation of the transmission map may prompt a few mutilations, for example, square antiquities. The patch-based dark channel figuring prompts a noisy transmission map. This is fundamental because of the presumption that t is a consistent incentive in a local patch. This isn't, in every case, genuine, mainly when the patch contains a sharp edge. This off-base supposition prompts clear edge artifacts. To get a refined map, numerous strategies have been utilized.

Refinement of transmission map: The transmission map generated appears pixilated on account of the pixel-based operation. If used in equation 1 to recover the scene radiance, the final Denoised image will thus look pixilated. This transmission map has to be smoothened. It can be observed that the dark channel of the noisy image is not dark, whereas the same dark channel image in the case of a clear image is relatively darker. This image of whiteness observed in the dark channel image of the noisy image is utilized to derive the depth map. The transmission map is the inverse of the dark channel image. This transmission map corresponds to the amount of light that travels from the object and reaches the camera plane in the presence or absence of noise. The noise in the propagation path loss is the amount of scene information reaching the camera, and darker is the transmission map.

These improving calculations have been applied legitimately on the transmission map. Notwithstanding, different calculations apply a pre-preparing upgrading calculation to the noisy image so as to forestall the transmission map from obscure and incorrect surfaces. The image noise model's main goal is to get J(x) from $I(x), A, and\ t(x)$, respectively. The J(x) is derived from eq. (1) which is given by equation (4)

$$J^c(x) = \frac{I^c(x) - A^c}{t_{pa}(x)} + A^c \quad (4)$$

The pixel and patch wise estimate determine the global road atmospheric light A^c and transmission map $t_{pa}(x)$. The dark channel is evaluated using the fact that dark pixels in noise-free pictures, with the exception of road areas, have an intensity value near to zero in at least one colour channel within an image patch. Shades of roadside automobiles, buildings, foliage, trees, and colourful and dark objects or surfaces cause low intensity values in non-road locations. Equation 5 is used to calculate the black pixel intensity value at a given spatial location in an arbitrary picture Jc(x) (5)

$$J^{dark}(x) = \min_{y \in \Omega(x)} [\min_{C \in [r,g,b]} J^c(y)] \quad (5)$$

As a result, the least intensity value in (x) among three channels r, g, and b is defined as the pixel intensity value in the dark channel picture $J^{dark}(x)$. If $J^c(y)$ is a noise-free picture, equation (6) suggests that dark pixels will be reduced and tentatively reduced to zero.

$$J^{dark} \rightarrow 0 \quad (6)$$

B. Noise Atmospheric Light Estimation

The primary concept behind the noise atmospheric light (A) estimate is to find the most blurred region in a foggy image. Transmission map estimation is used to detect this region because, as previously indicated, it offers a decent estimate of the noise thickness. First, the top 0.1 percent bright pixels of a noisy image's dark channel are determined. The highest intensity pixels in the input picture are then found among these pixels. These pixels, in reality, made up the fuzziest region and were regarded as noise-ambient light. It is the method of removing additional and unrealistic color casts produced by the environment. Other color casts are introduced in an atmospheric noise environment due to scattering and wavelength-selective absorption. The most common and widely used noise atmospheric light estimation algorithm is the gray world theory. If the weather is noisy, the brightest pixels in the noisy image are judged to be the most noise-opaque, and the sunlight represented by s is discarded in favor of noise atmospheric light.

This operation mainly focuses on the estimation of air light values for generation of transmission matrix. In the first step color image is converted into three indexes such as red, green and blue color channels such as $\{A^R, A^G, A^B \in A^c\}$. Then extract the low intensity pixels by using the color division approach, for satellite images cluster count will be more and vice versa for normal images. Then the clusters must be rearranged for the new transmission map estimation. Depending upon the air light values these clusters will be divided into three weight of each color channels (W_R,W_G and W_B). Then air light values (A_R,A_G and A_B)) will be generated based on updating of old air light values as show in Fig. 2.

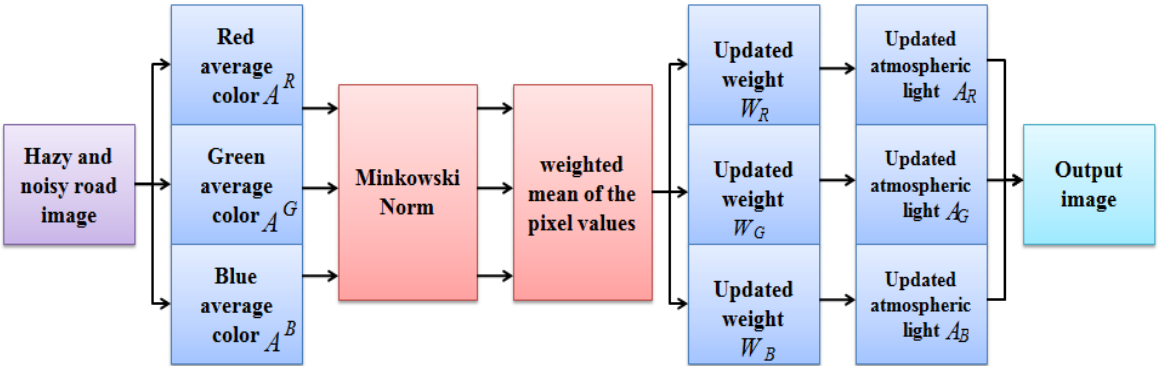

Fig. 2. Process of noise atmospheric light estimation

This work uses the shade of the GWO algorithm based on the Minkowski normalization to perform the noise atmospheric light estimation process. The Minkowski norm is utilized to normalize the output and produce the estimated lit picture. The Minkowski norm calculates a weighted mean of the pixel values and gives higher intensities more weight. This algorithm is based on the property that the image's average color is gray. These conditions do not hold by the noisy images because as the depth of the noise increases, the red channel of the image attenuates faster than the other color channels. This algorithm's proposed weight function is based on the Minkowski-norm and is defined using the formula below:

$$W_R = (\sum\sum((I^R(x))^P . M)^{\frac{1}{P}} \quad (7)$$

$$W_G = (\sum\sum((I^G(x))^P . M)^{\frac{1}{P}} (8)$$

$$W_B = (\sum\sum((I^B(x))^P . M)^{\frac{1}{P}} (9)$$

Here, $I^R(x)$, $I^G(x)$and $I^B(x)$represent the red, green, and blue channels of the red noisy image. M represents a mask which contains noise atmospheric light saturated pixels. "P" represents the minkowski norm. Shades of gray algorithm give the best result when the value of p is equal to 6. And W_R,W_G and W_B, are enhanced red channel, green channel and blue channel weights respectively.

The red, green, and blue channels of the red noisy picture are represented by $I^R(x)$, $I^G(x)$and $I^B(x)$. The M is a mask that contains noise and light-saturated pixels from the atmosphere. The minkowski norm is denoted by

the "*P*". When the value of p is equal to 6, the Shades of Gray algorithm produces the best results. And increased red channel, green channel, and blue channel weights are W_R,W_G and W_B, respectively.

$$S = \sqrt{({W_R}^2 + {W_G}^2 + {W_B}^2)} \quad (10)$$

Here, $S$is the root sum square of W, and Wbindicates weighted mean of the pixel values. Then noise atmospheric light channels are normalized using S and weights and generates the new noise atmospheric light levels as follows:

$$A_R = \frac{W_R}{S}, A_G = \frac{W_G}{S}, A_B = \frac{W_B}{S} \quad (11)$$

The updated noise atmospheric light red channel, green channel, and blue channel are represented by A_R , A_G and A_B , respectively. Finally, utilising three colour channels, the proposed method calculates the light enhanced output image as follows:

$${I_{new}}^R = \frac{I^R}{A_R.\sqrt{3}}, {I_{new}}^G = \frac{I^G}{A_G.\sqrt{3}}, {I_{new}}^B = \frac{I^B}{A_B.\sqrt{3}} \quad (12)$$

C. Multi-scale Optimal Fusion Denoising Model

The multi-scale fusion technique improves the visibility of poorly illuminated areas by using a multi-scale fusion-based strategy. The fundamental principle of this method is extracting the best pixel and patch features from the Transmission map estimation and refined image and then applying the estimated perceptual-based qualities called weight maps to them and finally fusing them to form the enhanced output. In the fusion-based strategy, three inputs derived from the single image will be by two patch images and one-pixel wise image by using estimation of three weight maps is done. The exposedness weight map measures the exposedness of pixels not exposed to road atmospheric constraints.

Laplacian weight map assigns high values to textures as well as edges. Colour cast weight map, introduced newly, increases red channel value, thereby reducing color cast. The saliency weight map measures the amount of discernible concerning other pixels. These weight maps are computed and applied to both the derived inputs. This method is a per-pixel implementation. Fusion integrates essential information from several input pictures into a single image that is more informative and comprehensive than the individual input images. There are three weight maps based on the luminance channel and one based on the chrominance-red channel. The effective weight map from the three weight maps are combined by averaging the weight map values as mentioned in the following equations

$${W_{avg}}^k = \frac{1}{N}\sum_{i=1}^{N} {W_i}^k \quad (13)$$

$${W_{norm}}^k = \frac{{W_1}^k}{\sum_{i=2}^{N} {W_i}^k} \quad (14)$$

Two color-cast weight maps from the derived inputs are considered separately. As a result of this operation, two weight maps are obtained for each derived input. Then these weight maps are normalized as shown in equation (14). These are the two normalized weight maps for luminance and chrominance-red channel. Finally, they are fused using luminance channel and chrominance-red channel to obtain the fused image.

$$t_{mof}(x) = {W_{avg}}^k(x).t_{pi}(x) + {W_{norm}}^k(x).t_{pa}(x) \quad (15)$$

D. Fast Iterative Domain GIF

Smoothing of the output image takes place with the help of guided filters in several Denoising techniques. Others have utilized rather than the bilateral filter, which is fundamentally the same as guided convolution. However, pixels are dealt with depending on the close-by area and comparative qualities. The guided filter is a smoothing channel with edge protecting properties, and it has a superior activity close to the edges. Since the soft matting, this has been utilized in the transmission refining strategy.

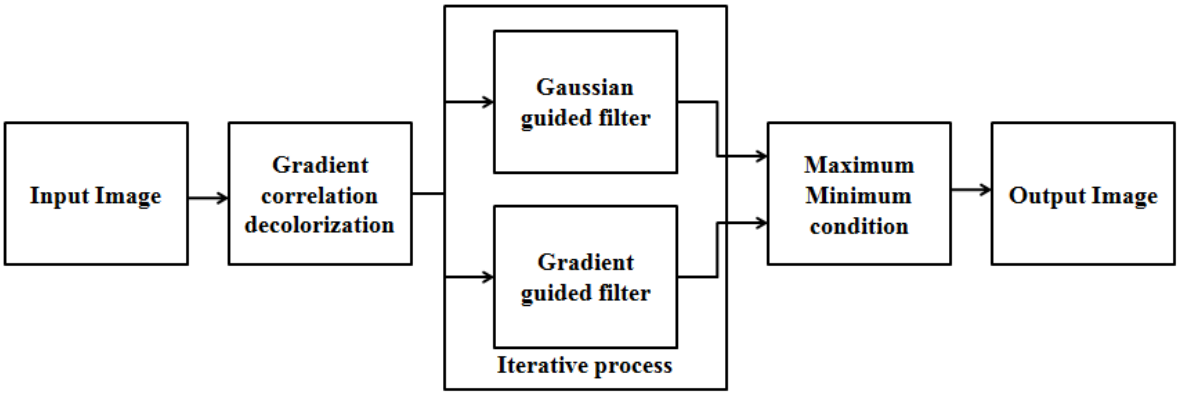

Fig. 3. Process of fast iterative domain GIF

In Fast ID-GIF, as shown in Fig. 3, the de-colorization operation will be performed to remove the white levels, or else excessive color levels will be removed here. For this purpose, three methods can be suitable: Gradient correlation, state contrast preserving de-colorization, and RGB to gray conversion. Among these three methods,

Gradient correlation de-colorization performs effectively because it provides the combined properties of pixel and patch transmission mapping. Here global and local contrasts are generated using image adjust methodologies. Global contrast will modify patch-level image properties; local is for pixel-level based on three new contrast levels. New color composites operations will be performed concerning the matrix's x and y-direction. Initialize the iterative environment and generate the new kernel matrix for every iteration. Thus, the updated kernel matrix will be convolved with the Gaussian guided filter and gradient guided filters every time. The maximum and minimum conditions will be applied to both filters using the absolute concept. After applying the maxima-minima conditions, the resultant output image will be generated by using the best properties of each filter patch, respectively.

E. Exposure Enhancing

Light temperature is increased or decreased when compared with the original image will be identified for further enhancement operations. By applying the light exposure or low light image enhancement concept, light levels will be automatically adjusted. Within the image, only the mean value is considered, then it is adjusted to the middle value only, finally resulting in the light enhanced output image.

IV. Simulation Results

This section deals with the detailed analysis of the simulations on various datasets. The three kinds of datasets are considered to evaluate the proposed work's performance: satellite life, synthesized, and noisy natural images. The qualitative and quantitative evaluation of the proposed work is compared with various state-of-the-art approaches such as ID-CNN [19], IDERS [29], and-MOF [25]. We compared our findings to those of other studies and then subjective analysis. Denoised results are compared to our technique using standard methods on synthetic and particular benchmark pictures.

A. Evaluations on Satellite Noisy Images

In the satellite dataset, 140 images are considered for the simulation. This is the remote sensing image dataset, so effective noise removed outcomes will generate by performing the experimentations on this dataset. The resultant output images will be helpful in further hyperspectral image segmentation and classification.

(a) (b) (c) (d) (e)

Fig. 4. (a) satellite input images (b) ID-CNN [19](c) IDERS [29] (d) TME-MOF [25] and (e) proposed denoised image

From Fig. 4, it is observed that each row represents experimentations on individual images, and columns are the Denoised output images of proposed and existing works, respectively. The figure shows that the existing works failed to remove the noise from input images, and the current works are suffering from the color casting (increasing) problems. Finally, the proposed method generates the perfectly Denoised output image with perfect color levels. Thus, it will cause to eliminate the crucial data of remote sensing satellite images.

B. Evaluations on Synthesized Noisy Images

The second category of datasets is manually synthesized from noisy images; for this purpose, 250 images are considered for experimentation. So, from this experimentation, the performance of the proposed method can be effectively analyzed, and subjective quality will be used as the reference standard.

(a) (b) (c) (d) (e)

Fig. 5. (a) synthesized input images (b) ID-CNN [19] (c) IDERS [29] (d) TME-MOF [25] and (e) proposed Denoised image

(a) (b) (c) (d)

Fig. 6. (a) satellite input images [19] (b) IDERS [29] (c) TME-MOF [25] and (d) proposed Denoised image

From Fig. 5, it is observed that each row represents experimentations on individual images, and columns are the Denoised output images of proposed and existing works, respectively. From the figure, it is observed that the current works are suffering from contrast and brightness-based problems. Hence the current works are failed to remove the noise from input images. Finally, the proposed method generates the perfectly Denoised output image with appropriate brightness, contrast, saturation, and hue levels.

C. Evaluation on Natural Noisy Images

There are two particular kinds of scenarios in the raw image datasets captured using high-definition cameras, and a total of 400 images are captured. The two scenarios are results in the indoor and outdoor datasets, respectively. These datasets help analyze the proposed method's performance under various noise atmospheric light scenarios. As the road atmospheric light changes, various works' proposed noise removing capacity changes differently. Thus, this experimentation gives a detailed analysis of road atmospheric light environments of indoor and outdoor scenarios as indoor datasets consist of low light levels or else contain artificial lights. In contrast, outdoor datasets consist of high excessive light levels.

From Fig. 6, it is observed that each row represents experimentations on individual images, and columns are the Denoised output images of proposed and existing works, respectively. The figure shows that the current works are suffering from the road atmospheric light-based problems. Hence the current works are failed to remove the road atmospheric-related environment hazards from the noisy input images on both indoor and outdoor datasets. Finally, the proposed method generates the perfectly Denoised output image with effective removal of atmospheric road lights and environmental hazards.

D. Comparison of Complexities

To evaluate the proposed method's performance, qualitative evaluation was carried out using the various complete reference image quality assessments (FRIQA) metrics. The FRIQA metrics are feature similarity index for color image (FSIMc), visual signal-to-noise ratio (VSNR), structural similarity index (SSIM), and peak signal-to-noise ratio (PSNR), respectively. The FRIQA metrics are compared with the state of art approaches for analyzing the proposed method quality standards.

The Table I shows that the proposed method gives the enhancive performance both quality-wise (PSNR & VSNR) and similarity-wise (SSIM & SSIM) for various datasets. The proposed method gives better performance compared to the ID-CNN[19], IDERS [29], and TME-MOF[25], respectively.

TABLE I: PERFORMANCE OF PROPOSED DEHAZING APPROACH WITH CONVENTIONAL APPROACHES

Dataset	Metric	ID-CNN [19]	IDERS [29]	TME-MOF [25]	Proposed
Satellite noisy images	**PSNR**	13.247	14.218	16.888	**21.918**
	VSNR	7.783	10.355	11.163	**14.317**
	SSIM	0.590	0.758	0.775	**0.914**
	FSIMc	0.813	0.856	0.916	**0.933**
	Running time (sec)	14.901	9.553	7.468	**6.612**
synthesized noisy images	**PSNR**	13.057	14.132	15.307	**17.420**
	VSNR	5.200	7.223	6.268	**15.429**
	SSIM	0.55	0.613	0.801	**0.955**
	FSIMc	0.774	0.808	0.855	**0.905**
	Running time (sec)	12.918	11.091	9.655	**5.225**
Indoor and outdoor noisy images	**PSNR**	16.464	14.336	17.659	**23.536**
	VSNR	10.812	9.337	11.259	**18.889**
	SSIM	0.616	0.795	0.817	**0.939**
	FSIMc	0.794	0.916	0.928	**0.945**
	Running time (sec)	16.536	13.889	9.426	**4.205**

V. CONCLUSION

Existing denoising algorithms have shown impressive results, but they have failed to assess ambient noise and atmospheric light in road pictures accurately. They merely expand the dazzling pixel approach locally in daylight denoising. According to the road atmospheric scattering model, the ambient noisy atmospheric light is close to the road zone's bright pixels. This study proposes a fusion-based technique that improves picture quality by eliminating noise and maintaining the original image's cool color tone to address these issues. To do this, the identical input picture is initially subjected to two simultaneous phases of dark channel prior based transmission map estimation and refinement, one for each pixel and one for each patch. Second, these pictures go through various versions of Exposure Fusion (depending on their Enhancement step), using the GWO algorithm Denoising. Using the ID-GIF method, both fusion processes' outputs are averaged out to create an underexposed noise-free image. Finally, to obtain a final improved noise-free image, the brightness of this noise-free image is boosted by approximating the brightness of the original image. The simulations are carried out on synthetic and real-time datasets such as noisy satellite images, synthesized noisy images, and noisy natural images with indoor and outdoor databases. The results show that the proposed method provides the better visual quality of output image and also provides the enhancive quality metrics compared to the various literature such as ID-CNN [19], IDERS [29], and TME-MOF [25], respectively.

Conflict of Interest

The authors declare no conflict of interest.

Author's Contribution

D. Subhashini carried out the literature study, participated in the sequence alignment, development of the method, statistical analysis and drafted the manuscript.

Dr. VBS Srilatha Indira Dutt participated in the development of proposed method and performed the statistical analysis.

References

[1] D. Subhashini and V. S. I. Dutt, "A review on road extraction based on neural and non-neural networks," *International Journal of Engineering Research and Technology*, vol. 9, no. 6, 2020.

[2] L. Pardthaisong, *et al.*, "Haze pollution in Chiang Mai, Thailand: A road to resilience," *Procedia Engineering*, vol. 212, pp. 85-92, 2018.

[3] N. Dat, G. D. Lee, and B. Kang, "Improved color attenuation prior for single-image haze removal," *Applied Sciences*, vol. 9, no. 19, p. 4011, 2019.

[4] N. Dat, S. Lee, and B. Kang, "Robust single-image haze removal using optimal transmission map and adaptive atmospheric light," *Remote Sensing*, vol. 12, no. 14, p. 2233, 2020.

[5] B. Ganguly, *et al.*, "Single image haze removal with haze map optimization for various haze concentrations," *IEEE Transactions on Circuits and Systems for Video Technology*, 2021.

[6] W. Yao, *et al.*, "Haze removal algorithm based on single-images with chromatic properties," *Signal Processing: Image Communication*, vol. 72, pp. 80-91, 2019.

[7] K. Chunghun and G. Kim, "Single image haze removal method using conditional random fields," *IEEE Signal Processing Letters*, vol. 25, no. 6, pp. 818-822, 2018.

[8] D. Akshay and S. Murala, "RYF-Net: Deep fusion network for single image haze removal," *IEEE Transactions on Image Processing*, vol. 29, pp. 628-640, 2019.

[9] B. Arianna, *et al.*, "Analysis of road-user interaction by extraction of driver behavior features using deep learning," *IEEE Access*, vol. 8, pp. 19638-19645, 2020.

[10] D. Akshay and S. Murala. "RYF-Net: Deep fusion network for single image haze removal," *IEEE Transactions on Image Processing*, vol. 29, pp. 628-640, 2019.

[11] D. Akshay, H. S. Aulakh, and S. Murala, "Ri-gan: An end-to-end network for single image haze removal," in *Proc. IEEE/CVF Conference on Computer Vision and Pattern Recognition Workshops*, 2019.

[12] Y. Chia-Hung, C. H. Huang, and L. W. Kang, "Multi-scale deep residual learning-based single image haze removal via image decomposition," *IEEE Transactions on Image Processing*, vol. 29, pp. 3153-3167, 2019.

[13] Z. Shengdong, F. He, and W. Ren, "NLDN: Non-local dehazing network for dense haze removal," *Neurocomputing*, vol. 410, pp. 363-373, 2020.

[14] N. Dat, S. Lee, and B. Kang, "Robust single-image haze removal using optimal transmission map and adaptive atmospheric light," *Remote Sensing*, vol. 12, no. 14, p. 2233, 2020.

[15] S. Liang, *et al*., "Deep joint rain and haze removal from a single image," in *Proc. 24th International Conference on Pattern Recognition (ICPR)*, 2018.

[16] C. Xinqiang, *et al*., "High-resolution vehicle trajectory extraction and denoising from aerial videos," *IEEE Transactions on Intelligent Transportation Systems*, vol. 22, no. 5, pp. 3190-3202, 2020.

[17] A. Cosmin, *et al*., "I-HAZE: A dehazing benchmark with real hazy and haze-free indoor images," in *Proc. International Conference on Advanced Concepts for Intelligent Vision Systems*. Springer, Cham, 2018.

[18] G. Soham, M. T. Asif, and L. Wynter, "Denoising autoencoders for fast real-time traffic estimation on urban road networks," in *Proc. IEEE 56th Annual Conference on Decision and Control (CDC)*, 2017.

[19] M. Mamta, *et al*., "IoT based image defogging system for road accident control during winters," in *Proc. 5th International Conference on Computing, Communication and Security (ICCCS)*, 2020.

[20] N. Dat and B. Kang, "A new data preparation methodology in machine learning-based haze removal algorithms," in *Proc. International Conference on Electronics, Information, and Communication (ICEIC)*, 2019.

[21] T. Shanshan and H. Yu, "Application of bounded total variation denoising in urban traffic analysis," arXiv preprint arXiv:1808.03258, 2018.

[22] C. Xinqiang, *et al*., *Extracting and Denoising Vehicle Trajectory Automatically from Aerial Roadway Surveillance Videos*, No. 19-03147. 2019.

[23] K. Minsub, *et al*., "Single image dehazing of road scenes using spatially adaptive atmospheric point spread function," *IEEE Access*, vol. 9, pp. 76135-76152, 2021.

[24] L. Kunming, *et al*., "Photo-realistic simulation of road scene for data-driven methods in bad weather," in *Proc. IEEE International Conference on Computer Vision Workshops*, 2017.

[25] K. Minsub, S. Hong, and M. G. Kang, "Single image haze removal using multiple scattering model for road scenes," *Electronic Imaging*, vol. 2020, no. 16, pp. 81-1, 2020.

[26] F. Wang and W. Weixing, "Road extraction using modified dark channel prior and neighborhood FCM in foggy aerial images," *Multimedia Tools and Applications*, vol. 78, no. 1, pp. 947-964, 2019.

[27] W. Qianqian, *et al*., "Automatic estimation of road visibility in foggy weather based on image feature statistics," *Journal of Electronic Imaging*, vol. 30, no. 5, 2021.

[28] H. Lin-Yuan, J. Z. Zhao, and D. Y. Bi, "Effective haze removal under mixed domain and retract neighborhood," *Neurocomputing*, vol. 293, pp. 29-40, 2018.

[29] D. Subhashini and V. B. S. S. I. Dutt, "An innovative hybrid technique for road extraction from noisy satellite images," *Materials Today: Proceedings*, 2021.

D. Subhashini is currently working as Asst. Professor in Department of ECE at Mahatma Gandhi Institute of Technology, Hyderabad, India. Her area of research is Image Processing and Digital Systems design. She has 15 publications in various national and International Journals. She has 16 Years of teaching experience. She is currently pursuing her Ph.D. degree from GITAM University, Visakhapatnam.

Srilatha Indira Dutt Vemuri is currently working as Professor in Department of ECE at, GITAM University, Visakhapatnam, India. Her areas of research are Communication Networks Global Navigation Satellite Systems and Satellite Communication. She has more than 90 publications in various national and international conferences and Journals.